Research Square

Preprints are preliminary reports that have not undergone peer review.
They should not be considered conclusive, used to inform clinical practice,
or referenced by the media as validated information.

# Optimizing Physiological Image Compression via Discrete Wavelet Transform without Loss of Clinical Relevance

**Dawit Teklu Weldeslasie**

dawit.tekulu@gmail.com

Aksum University

**Tedros Kebede Bidada**

Aksum University

**Yayneshet Tadele Aynalem**

Axum Polytechnic College

**Research Article**

**Keywords:** Physiological image compression, discrete wavelet transform, compression ratio, peak signal-to-noise ratio, picture quality scale, clinical relevance

**Posted Date:** September 2nd, 2026

**DOI:** https://doi.org/10.21203/rs.3.rs-10458159/v1

**License:** This work is licensed under a Creative Commons Attribution 4.0 International License.
Read Full License

**Additional Declarations:** No competing interests reported.

# Optimizing Physiological Image Compression via Discrete Wavelet Transform without Loss of Clinical Relevance

Dawit Teklu Weldeslasie[1*] https://orcid.org/0009-0000-5388-5197, Tedros Kebede Bidada[2], Yayneshet Tadele Aynalem[3]

[1]Aksum University, Aksum, Ethiopia, Department of Information Technology
[2]Aksum University, Aksum, Ethiopia, Department of Computer Science
[3]Axum Polytechnic College, Aksum, Ethiopia, Department of Information Technology

*Corresponding author(s). E-mail(s): dawit.tekulu@gmail.com
Contributing authors: ted32t@gmail.com , yayneshettadele@gmail.com

**Abstract**

The rapid advancement of digital technologies has led to an exponential increase in the volume of image data, creating significant challenges for efficient storage, transmission and retrieval. Image compression has therefore become an essential technique for reducing storage requirements while preserving image quality. Wavelet transforms provide an effective mathematical framework for representing image information at multiple levels of resolution, enabling efficient approximation and compression with reduced data redundancy. This study presents a two-dimensional (2D) image compression method based on the Haar wavelet, the most computationally efficient wavelet transform. The proposed approach employs the two-dimensional Discrete Wavelet Transform (2D-DWT) to decompose the input image into approximation and detail coefficients. The compressed image is subsequently reconstructed using the retained approximation and estimated detail coefficients. The performance of the compression method is evaluated using standard image quality metrics, including Compression Ratio (CR), Peak Signal-to-Noise Ratio (PSNR), and Picture Quality Scale (PQS). The proposed method demonstrates effective compression while maintaining acceptable reconstructed image quality. Furthermore, the study highlights the relevance of wavelet-based compression in medical imaging, where efficient storage and transmission must be achieved without compromising significant image information. Although lossy compression techniques generally provide higher compression ratios, their adoption in medical imaging remains limited because of diagnostic concerns. Consequently, the primary objective of the study was to maximize compression efficiency while preserving clinical relevance and ensuring diagnostic reliability. Hence, the Haar wavelet becomes a promising solution for resource-constrained environments because of its ease of implementation and computational efficiency.

**Keywords**: Physiological image compression, discrete wavelet transform, compression ratio, peak signal-to-noise ratio, picture quality scale, clinical relevance

## 1. Introduction to the study

The rapid growth of digital technologies and web-based services has significantly increased the volume of digital image data generated, stored and transmitted across various applications. Consequently, efficient image compression has become essential for reducing storage requirements, accelerating data transmission over bandwidth-limited networks, and improving the efficiency of image retrieval systems. These requirements are particularly important in applications such as medical imaging, remote sensing, multimedia systems, and cloud-based image repositories, where large image datasets are routinely processed [1,2].

Image compression techniques aim to reduce data redundancy while preserving the visual quality and essential information contained in the original image. In addition to minimizing storage space and transmission time, effective compression techniques provide progressive or incremental transmission capabilities, allowing coarse image representations to be transmitted first, followed by finer details as additional data become available. This feature is particularly valuable in web-based applications and real-time image communication systems [2,3].

Among the various image compression approaches, wavelet-based methods are one of the most effective techniques because of their ability to represent images at multiple resolutions. Unlike the Discrete Cosine Transform (DCT), which processes images in independent blocks and may introduce blocking artifacts at high compression ratios, wavelet transforms analyze the entire image using multiresolution decomposition. This property enables superior energy compaction, reduces visual artifacts, and preserves important image features more effectively [4,5].

Wavelet compression is based on multiresolution analysis, where an image is decomposed into approximation and detail components at different frequency levels. Similar to conventional JPEG compression, the transformed image is represented by a set of coefficients. However, most wavelet coefficients are either very small or close to zero, allowing insignificant coefficients to be discarded while retaining only the most informative components. As a result, high compression ratios can be achieved with minimal degradation in reconstructed image quality [4,5].

Among the available wavelet families, the Haar wavelet is computationally most efficient transform. Its low computational complexity, ease of implementation, and fast decomposition and reconstruction processes make it particularly suitable for real-time image compression applications and systems with limited computational resources. Despite its simplicity, the Haar wavelet provides satisfactory compression performance while preserving important image characteristics [5,6].

This study investigates a two-dimensional (2D) image compression approach based on the Haar Discrete Wavelet Transform (DWT). The proposed method performs multiresolution image decomposition, reconstructs the compressed image using the approximation and selected detail coefficients, and evaluates

compression performance using widely accepted quality metrics, including Compression Ratio (CR), Peak Signal-to-Noise Ratio (PSNR), and Picture Quality Scale (PQS). The findings demonstrate the effectiveness of Haar wavelet-based compression as a low-complexity and reliable solution for efficient image storage and transmission while maintaining acceptable reconstructed image quality.

## 2. State of the art in the field

Wavelet transform has become one of the most influential techniques in modern image processing because of its ability to represent image information at multiple spatial resolutions. Unlike conventional transform-based methods, wavelet analysis decomposes an image into approximation and detail components, enabling efficient representation of both low- and high-frequency information. This multiresolution property has made wavelet transforms a fundamental tool in image compression, denoising, feature extraction, segmentation, and image enhancement [7-9].

Among the numerous transform-based image compression techniques, wavelet-based methods have demonstrated acceptable performance, particularly at medium and high compression ratios. Earlier image coding standards, such as JPEG, employ the Discrete Cosine Transform (DCT), which processes images in independent blocks and often introduces blocking artifacts when high compression ratios are applied. In contrast, wavelet-based compression analyzes the entire image without block partitioning, thereby reducing visual artifacts and preserving structural image information more effectively. These advantages led to the adoption of wavelet technology in the JPEG image compression standard [8-10].

Wavelet-based image compression offers several important advantages. First, multiresolution decomposition enables progressive image transmission, allowing low-resolution representations to be reconstructed before finer details are received. Second, wavelet coding produces fewer visual artifacts than block-based methods, resulting in improved subjective image quality. Third, wavelet transforms exhibit excellent energy compaction, where most of the signal energy is concentrated in a relatively small number of coefficients, facilitating efficient compression. Furthermore, wavelet-based methods are more robust to transmission errors and provide flexible control over compression quality and bit rate, making them suitable for web-based multimedia applications, remote sensing, and medical imaging systems [8-11].

The effectiveness of wavelet compression largely depends on the selected wavelet family. Among the available wavelets, the Haar wavelet remains one of the most computationally efficient transforms. Although more sophisticated wavelets, such as Daubechies, Symlets, and Coiflets, generally provide higher energy compaction, the Haar wavelet offers significant advantages in terms of computational simplicity, rapid decomposition and reconstruction, and ease of implementation. Consequently, it remains an attractive choice for real-time applications and systems with limited computational resources [11,12] of the low income countries.

### 2.1 Digital images maintaining acceptable visual fidelity

A digital image is a two-dimensional function, (f(x,y)), where (x) and (y) denote spatial coordinates and the function value represents the intensity or gray level at each location. Following image acquisition, the continuous image is converted into a discrete representation through two fundamental processes; spatial sampling and gray-level quantization. Sampling divides the image into a finite number of pixels, while quantization assigns each pixel an integer intensity value. The resulting image can therefore be represented as a two-dimensional matrix whose elements correspond to individual pixel intensities [13].

The quality of a digital image depends on the sampling resolution and the number of quantization levels. Higher spatial resolution and finer quantization provide a more accurate representation of the original scene but also increase storage requirements. Consequently, efficient image compression techniques are essential for reducing data redundancy while maintaining acceptable visual quality [8,13].

### 2.2 Digital image processing algorithms

Digital image processing involves manipulating digital images using computational algorithms to improve image quality, extract useful information, or reduce data redundancy. Since computers operate on numerical data, continuous images must first undergo digitization before further processing. The digitized image is represented as a matrix of pixel intensity values, enabling mathematical operations such as enhancement, restoration, segmentation, feature extraction, and compression [13,14].

Image compression is one of the most important applications of digital image processing. By exploiting spatial and statistical redundancy within image data, compression algorithms significantly reduce storage space and transmission bandwidth while preserving the visual and structural characteristics required by the target application. Wavelet compression has become particularly attractive because of its multiresolution representation, high compression efficiency, and ability to reconstruct images with minimal perceptual distortion [8-11].

## 3. Methodology and system framework

This study implements a two-dimensional (2D) image compression framework based on the Haar Discrete Wavelet Transform (DWT). The methodology consists of image decomposition, coefficient quantization, entropy coding, and image reconstruction. The proposed framework was designed to reduce image redundancy while preserving the visual information required for accurate image reconstruction [17].

### 3.1 Image compression system framework

The implemented lossy image compression system comprises three major components (i) transform coding, (ii) quantization, and (iii) entropy encoding [17,18]. The transform stage converts the original image into

another domain in which most of the image energy is concentrated in a relatively small number of coefficients. The transformed coefficients are subsequently quantized to reduce data precision and achieve compression. Finally, entropy coding was applied to eliminate statistical redundancy and further reduce the compressed bitstream size without introducing additional information loss. Fig 1 illustrates the general architecture of the proposed image compression framework.

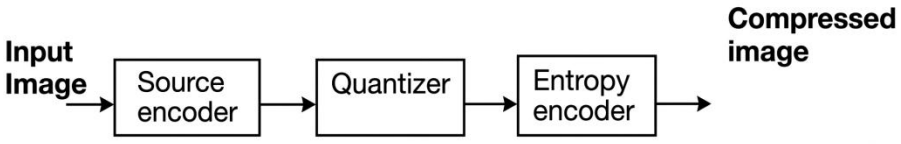



Fig.1 the image compression framework

Various transform techniques have been developed for image compression, including the Discrete Fourier Transform (DFT), Discrete Cosine Transform (DCT), and Discrete Wavelet Transform (DWT). Among these techniques, the DWT provides multiresolution representation and generally produces better image quality at higher compression ratios [18,19].

### 3.2 Quantization process

Quantization is the primary source of compression in a lossy image coding system [18,20]. During this stage, the precision of the transformed coefficients is reduced by mapping a range of coefficient values to a smaller set of representative values. Since multiple input values are represented by a single output value, quantization introduces irreversible information loss but significantly decreases the number of bits required for storage.

Quantization methods are generally classified into scalar quantization (SQ) and vector quantization (VQ) [20]. Scalar quantization processes each transform coefficient independently, whereas vector quantization operates on groups of coefficients simultaneously. Depending on the application requirements, either uniform or non-uniform quantization strategies may be employed to balance compression efficiency and reconstructed image quality.

### 3.3 Entropy encoding for representation methods

After quantization, entropy encoding was performed to remove the remaining statistical redundancy [18,21] from the compressed data without further degrading image quality. Entropy encoders assign shorter codewords to frequently occurring symbols and longer codewords to less frequent symbols, thereby minimizing the average number of bits required to represent the compressed data.

Common entropy coding techniques include Huffman coding, arithmetic coding, and Run-Length Encoding (RLE). Huffman coding and arithmetic coding provide high compression efficiency, while RLE offers lower computational complexity and is particularly effective when long sequences of identical coefficients occur [21]. An efficient entropy encoder, together with an appropriate transform and quantization strategy, plays a significant role in maximizing the overall compression performance.

### 3.4 Haar wavelet transform method

The proposed image compression method employs the Haar wavelet because of its low computational complexity and efficient multiresolution representation [19,22]. The Haar wavelet is an orthogonal wavelet and forms the basis for many practical image compression algorithms. The applied Haar transform [16] decomposes an image into the following equations.

Definition 1, Let ø: R, R is defined by:

$$\phi(t) = \begin{cases} 1 & t \in [0,1) \\ 0 & t \notin [0,1) \end{cases} \quad (1)$$

Define $\phi_i^j : \mathbb{R} \to \mathbb{R}$ as,

$$\phi_i^j(t) = \sqrt{2^j}\phi(2^j t - i), j = 0, 1, \ldots \text{ and } i = 0, 1, \ldots, 2^j - 1. \quad (2)$$

Define the vector space Vj as,

$$V^j = sp\{\phi_i^j\}_{i=0,\ldots,2^j-1} \quad (3)$$

Where, sp denotes the linear span of the set of scaling functions. The index j refers to dilation and i refer to translation index of the scaling function. This definition may be different for different literature. Sometimes one defines the scaling function for negative integers as well and uses a different sign convention. Whenever we use a text on wavelets, we make sure we know what sign convention is being used.

The constant $\sqrt{2i_j}$ is chosen such that $\langle \phi_i^j, \phi_i^j \rangle = \int_0^1 \phi_i^j(t)^2 dt = 1$. If one considers the scaling function on other intervals than [0, 1], the normalization constant will change.

Definition 2, (the Haar wavelet function); Let $\phi_i^j : \mathbb{R} \to \mathbb{R}$ be defined by:

$$\psi(t) = \begin{cases} 1 & t \in [0, 1/2) \\ -1 & t \in [1/2, 1) \\ 0 & t \notin [0,1) \end{cases} \quad (4)$$

Define $\phi_i^j : \mathbb{R} \to \mathbb{R}$ as,

$$\psi_i^j(t) = \sqrt{2^j}\psi(2jt - i),\ j = 0, 1, \ldots \text{and } i = 0, 1, \ldots, 2^j - 1\,. \quad (5)$$

Define the vector space Wj,

$$W^j = sp\{\psi_i^j\}_{i=0,\ldots,2^j-1} \quad (6)$$

Where, sp denotes the linear span. It should be noted that the notation used to define the scaling functions may vary across the wavelet foundation. Again, when implementing wavelet algorithms, it is important to ensure consistency with the notation and conventions adopted in the selected reference. Therefore, the constant is chosen such that:

$$\sqrt{2^j}\,\langle \psi_i^j, \psi_i^j \rangle = \int_0^1 \psi_i^j(t)^2\,dt = 1 \quad (7)$$

When the Haar wavelet function is defined over intervals other than [0,1], the corresponding normalization constant must be adjusted accordingly to preserve the orthonormality of the basis functions. So, the structure of the Haar basis has important property that:

$$V^{j+1} = V^j \oplus W^j\,. \quad (8)$$

In the above equation of wavelet transformation of a signal, we consider a signal with 8 samples for clarity. However, the procedure can be generalized to any finite signal. The analysis simplifies if the length (dimension) of the signal for some positive integer. So, Let $f \in \mathbb{R}^8$ and expand this signal into $V^0 \oplus W^0 \oplus W^1 \oplus W^2$ spanned by the basis vectors according to Definitions 1 and 2 (discretized), then;

$$\begin{aligned} f = {} & \langle f, \phi_0^0 \rangle\, \phi_0^0 + \langle f, \psi_0^0 \rangle\, \psi_0^0 + \langle f, \psi_0^1 \rangle\, \psi_0^1 + \\ & < \langle f, \psi_0^1 \rangle\, \psi_0^1 + < \langle f, \psi_1^1 \rangle\, \psi_1^1 + \\ & < \langle f, \psi_0^2 \rangle > \psi_0^2 + \langle f, \psi_1^2 \rangle\, \psi_1^2 + \langle f, \psi_2^2 \rangle\, \psi_2^2 + \langle f, \psi_3^2 \rangle\, \psi_3^2. \end{aligned} \quad (9)$$

Analogous to the Fourier expansion of a signal, the wavelet representation [16] was obtained by computing the corresponding inner products $< f, \phi_i^j >$ and $< f, \phi_i^j >$ with the scaling and wavelet basis functions. However, in practical implementations, the computation of the wavelet coefficients is performed using efficient algorithms, as described in the following subsection.

3.5 The wavelet transform decomposition and reconstruction

To illustrate the operation of the Haar wavelet transform [22], consider a simple one-dimensional (1D) image consisting of four pixels with intensity values [9,7,3,5]. The Haar wavelet basis represents this signal by computing its wavelet transform through a multiresolution decomposition process. The first step is to calculate the pairwise averages of adjacent pixel values, producing a lower-resolution representation of the original signal. For the above case, the resulting averaged values are [8,4]. Although this averaging process reduces the data size, it also discards part of the original information. To enable perfect reconstruction of the original signal, the lost information is preserved in the form of detail coefficients.

In this example, the first detail coefficient is assigned a value of 1, indicating that the average value of 8 is one unit smaller than the first pixel value (9) and one unit larger than the second pixel value (7). Similarly, the remaining detail coefficients are computed for the other pixel pairs. By combining the approximation coefficients with the corresponding detail coefficients, the original four-pixel signal can be reconstructed without information loss. The above procedure can be mathematically expressed as follows:

$$Wf = \frac{1}{\sqrt{2}}\left(\frac{35}{2}\phi_0^0 + \frac{13}{2}\psi_0^0 - \frac{-10}{\sqrt{2}}\psi_0^1 + \frac{11}{\sqrt{2}}\psi_1^1 - 3\psi_0^2 - 1\psi_1^2 + 3\psi_2^2 - 2\psi_3^2\right) \quad (10)$$

Where, W is the wavelet transform. This single number is used to recover the first two pixels of our original four-pixel image. Similarly, the second detail coefficient is -1, since 4 + (-1) = 3 and 4 - (-1) =5. Thus, the original image is decomposed into a lower resolution (two-pixel) version and a pair of detail coefficients. Repeating this process recursively on the averages gives the full decomposition shown in Table 1.

Table 1, Decomposition process of image data into lower resolution levels

| **Resolution** | **Averages** | **Detail Coefficients** |
|---|---|---|
| 4 | [9 7 3 5] | |
| 2 | [8 4] | [1 -1] |
| 1 | [6] | [2] |

For the one-dimensional Haar basis, the wavelet transform of the original four-pixel image is represented by the coefficient vector [6, 2, 1, −1]. The original image can be reconstructed at any desired resolution by recursively combining the approximation coefficients with the corresponding detail coefficients through inverse averaging and differencing operations. The extension of the Haar wavelet transform to two-dimensional (2D) image compression follows naturally from the one-dimensional case, where an image is represented as a sequence of wavelet coefficients. Alternatively, a one-dimensional image may be viewed

as a piecewise-constant function defined on the half-open interval [0,1). This interpretation provides the mathematical foundation for multiresolution analysis through the concept of vector spaces.

A one-pixel image corresponds to a function that is constant over the entire interval [0,1). Let V0 denote the vector space containing all such functions. Similarly, a two-pixel image consists of two constant segments defined over the intervals [0,1/2) and [1/2,1), and the corresponding vector space is denoted by V1. Extending this construction recursively, the vector space Vj contains all piecewise-constant functions defined on the interval [0,1), where each function is constant over each of the 2j equal subintervals. Consequently, every one-dimensional image containing 2j pixels can be regarded as an element (vector) of the space Vj. Since every function in Vj is also a piecewise-constant function in the finer-resolution space Vj+1, the vector spaces satisfy the nested relationship as follows:

$$V0 \subset V1 \subset V2 \subset \cdots .$$

This hierarchy of nested vector spaces forms the basis of multiresolution analysis (MRA), which is fundamental to wavelet theory. It guarantees that every function represented in a lower-resolution space can be represented exactly in any higher-resolution space. The converse, however, is generally not true. A function G(x) belonging to Vj+1cannot, in general, be represented exactly in the lower-resolution space Vj, since the finer-scale details are lost during approximation.

To represent functions within each vector space Vj, a corresponding set of basis functions is defined. These basis functions are known as scaling functions and are commonly denoted by $\phi$. For the Haar wavelet, a simple basis for Vj is obtained from scaled and translated box functions, which serve as the foundation for constructing the Haar multiresolution representation. The scaling functions are defined as follows:

$$\Phi 1\, j(x) := \varphi^{j}(2jx - i) \quad i = 0, 1, 2.....2j - 1 \qquad (11)$$

Where,

$$\varphi(x) := \begin{cases} 1 & \text{for } 0 \le x < 1 \\ 0 & \text{otherwise} \end{cases} \qquad (12)$$

The wavelets corresponding to the box basis are known as the Haar wavelets, given by $\Psi j1 := \Psi(2jx - i)$ i = 0, 1, 2…..2j -1 where,

$$\Psi(x) := \begin{cases} 1 \text{ for } 0 \le x < 1/2 \\ -1 \text{ for } 1/2 \le x < 1 \\ 0 \text{ otherwise} \end{cases} \qquad (13)$$

Thus, the DWT for an image as a 2D signal was obtained from 1D DWT. We get the scaling function and wavelet function for 2D by multiplying two 1D functions. The scaling function is obtained by multiplying two 1D scaling functions: $\varphi(x, y) = \varphi(x)\, \varphi(y)$. The wavelet functions are obtained by multiplying two

wavelet functions or wavelet and scaling function for 1D. For the 2D case, there exist three wavelet functions that scan details in horizontal $\Psi(1)(x,y)= \varphi(x)\Psi(y)$, vertical $\Psi(2)(x,y)= \Psi(x)\varphi(y)$ and diagonal directions: $\Psi(3)(x,y)=\Psi(x)\ \Psi(y)$. This is represented as a four channel perfect reconstruction filter bank as shown in Fig 2.

Now, each filter is 2D with the subscript indicating the type of filter (HPF or LPF) for separable horizontal and vertical components. By using these filters in one stage, an image was decomposed into four bands. There are three types of detail images for each resolution: horizontal (HL), vertical (LH), and diagonal (HH) [19,22,23]. The operations are repeated on the low low (LL) band using the second stage of identical filter bank. Thus, a typical 2D DWT used in an image compression generates the structure shown in Fig 3.

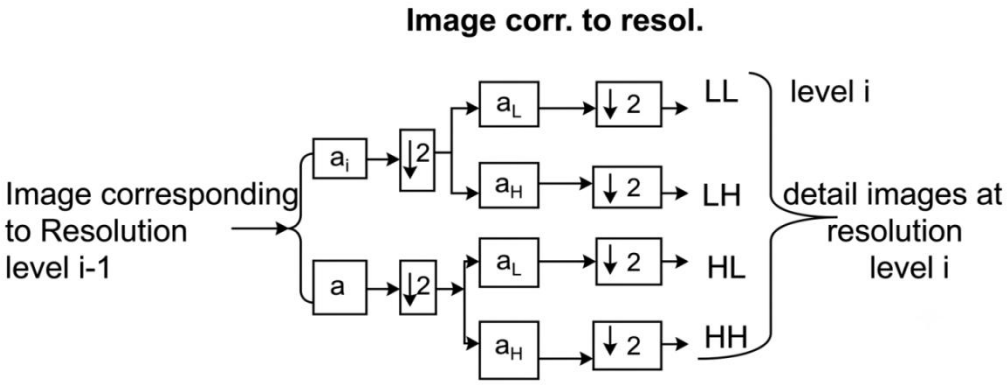



Fig.2 Single-level filter decomposition stage of the 2D discrete wavelet transform

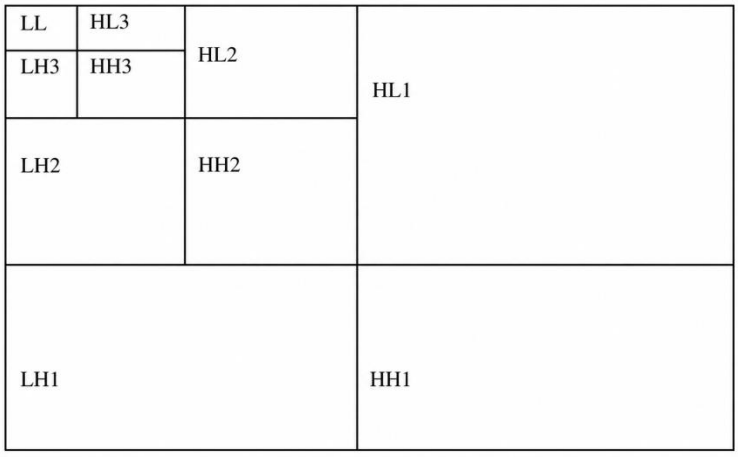



Fig. 3 Hierarchical structure of the wavelet decomposition process

The transformation of a two-dimensional (2D) image is a natural extension of the one-dimensional (1D) Haar wavelet transform described previously. In the first stage, the 1D Haar wavelet transform was applied independently to each row of the image matrix. This operation generates a set of approximation (average) coefficients together with the corresponding detail coefficients for every row [19].

The transformed rows are subsequently treated as a new image, and the 1D Haar transform is applied to each column [22]. This second transformation produces detail coefficients in both the horizontal and vertical directions, leaving a single approximation coefficient that represents the overall average of the image. To obtain a multiresolution representation, the decomposition process is recursively applied only to the sub-band containing the approximation coefficients until the desired decomposition level is reached.

To illustrate the procedure, the 2D Haar wavelet transform is applied to an 8×8 grayscale image, where each pixel is represented by an intensity value. The selected image segment, extracted from an anonymized image, is shown in Fig 4, while its corresponding matrix representation is presented in Fig 5. The Haar transform is computed by performing successive averaging and differencing operations on adjacent pixel values to obtain a more compact representation of the original image.

For example, considering the first row of the image matrix in Fig 5, the approximation coefficients are calculated as (64+2)/2=33, (3+61)/2=32, (60+6)/2=33, (7+57)/2=32. The corresponding detail coefficients are obtained by subtracting each approximation coefficient from the first element of its respective pixel pair as 64–33 =31, 3–32= –29, 60–33=27, 7–32= –25.

The same averaging and differencing operations are then applied to the remaining rows and columns of the image matrix. By recursively repeating this process on the approximation sub-band, the complete two-dimensional Haar wavelet decomposition is obtained, providing an efficient multiresolution representation suitable for image compression.



Fig.4 The 8 × 8 pixel dental image used for wavelet compression analysis

$$\begin{pmatrix} 64 & 2 & 3 & 61 & 60 & 6 & 7 & 57 \\ 9 & 55 & 54 & 12 & 13 & 51 & 50 & 16 \\ 17 & 47 & 46 & 20 & 21 & 43 & 42 & 24 \\ 40 & 26 & 27 & 37 & 36 & 30 & 31 & 33 \\ 32 & 34 & 35 & 29 & 28 & 38 & 39 & 25 \\ 41 & 23 & 22 & 44 & 45 & 19 & 18 & 48 \\ 49 & 15 & 14 & 52 & 53 & 11 & 10 & 56 \\ 8 & 58 & 59 & 5 & 4 & 62 & 63 & 1 \end{pmatrix} \quad (14)$$

Fig.5 Two-dimensional (2D) array representation of image intensity values

Consequently, the transformed first row is obtained as (33,32,33,32,31,−29,27,−25). The averaging operation is then recursively applied to the approximation coefficients, i.e., (33,32,33,32). Subsequently, the same averaging and differencing procedure is performed on the first two approximation coefficients of the newly transformed row. As a result, the final transformed row is given by (32.5,0,0.5,0.5,31,−29,27,−25).

Applying this procedure to every row of the image matrix shown in Fig 5 produces the intermediate transformed matrix presented in Fig 6. The same averaging and differencing operations are then applied to each column of the intermediate matrix to obtain the final transformed matrix, as illustrated in Fig 7.

The row-wise and column-wise transformations are recursively repeated according to the selected decomposition level; consequently, higher decomposition levels produce additional wavelet transformations. It is important to note that the upper-left element of Fig 7, namely 32.5, represents the single approximation coefficient corresponding to the overall average of all pixel values in the original image matrix. The remaining elements constitute the detail coefficients, which capture the horizontal, vertical, and diagonal variations within the image.

In MATLAB, the image is represented as a two-dimensional (2D) array, where each matrix element corresponds to the intensity value of a pixel. The objective of the wavelet transform is to exploit spatial redundancy by transforming the image into a domain in which regions with little or no variation are represented by coefficients with very small or zero values. The zero-valued coefficients observed in Fig 9 result from identical or nearly identical adjacent pixel values in the original image matrix.

For most image matrices, the corresponding wavelet-transformed representation is considerably sparser than the original image. Such sparse representations require less storage space and can be transmitted more efficiently because only the locations and values of the non-zero coefficients need to be stored or encoded. This property makes wavelet transforms highly effective for image compression applications by significantly reducing data redundancy while preserving the essential image information.

$$\begin{bmatrix} 32.5 & 0 & 0.5 & 0.5 & 31 & -29 & 27 & 25 \\ 32.5 & 0 & -0.5 & -0.5 & -23 & 21 & -19 & 17 \\ 32.5 & 0 & -0.5 & -0.5 & -15 & 13 & -11 & 9 \\ 32.5 & 0 & 0.5 & 0.5 & 7 & -5 & 3 & -1 \\ 32.5 & 0 & 0.5 & 0.5 & -1 & 3 & -5 & 7 \\ 32.5 & 0 & -0.5 & -0.5 & 9 & -11 & 13 & -15 \\ 32.5 & 0 & -0.5 & -0.5 & 17 & -19 & 21 & -23 \\ 32.5 & 0 & 0.5 & 0.5 & -25 & 27 & -29 & 31 \end{bmatrix} \quad (15)$$

Fig.6 Transformed array obtained after applying row-wise operations

$$\begin{bmatrix} 32.5 & 0 & 0 & 0 & 0 & 0 & 0 & 0 \\ 0 & 0 & 0 & 0 & 0 & 0 & 0 & 0 \\ 0 & 0 & 0 & 0 & 4 & -4 & 4 & -4 \\ 0 & 0 & 0 & 0 & 4 & -4 & 4 & -4 \\ 0 & 0 & 0.5 & 0.5 & 27 & -25 & 23 & -21 \\ 0 & 0 & -0.5 & -0.5 & -11 & 9 & -7 & 5 \\ 0 & 0 & 0.5 & 0.5 & -5 & 7 & -9 & 11 \\ 0 & 0 & -0.5 & -0.5 & 21 & -23 & 25 & -27 \end{bmatrix} \quad (16)$$

Fig.7 Final transformed matrix after one level of two-dimensional Haar wavelet decomposition

As illustrated in Fig. 7, the final transformed matrix contains a large number of zero-valued entries. From this transformed matrix, the original matrix can be easily reconstructed by applying the inverse operations of averaging and differencing. Therefore, the original image can be recovered from the transformed image without any loss of information. This process results in a lossless compression of the image.

However, to achieve a higher compression ratio, lossy compression must be applied. In this approach, a non-negative threshold value, denoted by ε, is selected. Any detail coefficient in the transformed data whose magnitude is less than or equal to ε is replaced with zero. This increases the number of zero entries in the transformed matrix, thereby improving the compression level. Hence, when ε = 0, the compression is lossless. When lossy compression is applied, an approximation of the original image can be reconstructed.

The selection of the threshold value is a critical factor because there is a trade-off between the value of ε and the quality of the compressed image. In this study, three different thresholding techniques are considered; hard thresholding, soft thresholding, and universal thresholding [15]. These thresholding methods are defined as follows:

$$\mathbf{T}_{i(\varepsilon,x)} = \begin{cases} 0, \text{if } |x| < \varepsilon \ldots\ldots\ldots \text{soft threshold} \\ sign(x)(|x| - \varepsilon), \text{otherwise} \end{cases} \quad \ldots\ldots\ldots\ldots\ldots\ldots (17)$$

$$T(\varepsilon,x) = \begin{cases} 0, \text{if } x < \sigma(2\log 2N)1/2 \\ x, \text{otherwise} \ldots\ldots \text{hard threshold} \end{cases} \quad \ldots\ldots\ldots\ldots\ldots\ldots\ldots (18)$$

$$T(\varepsilon,x) = \begin{cases} 0, \text{if } x < (2\log 2N)1/2 \\ x, \text{otherwise} \ldots\ldots \text{universal threshold} \end{cases} \quad \ldots\ldots\ldots\ldots\ldots\ldots (19)$$

Where σ represents the standard deviation of the wavelet coefficients, and N denotes the total number of wavelet coefficients. In general terms, the compression ratio of an image is determined by comparing the number of nonzero elements in the original matrix with the number of nonzero elements in the modified

transformed matrix. Usually, the main steps involved in 2D image compression using the Haar Wavelet as the basis function are, (a) begin with the matrix P representing the original image; (b) calculate the transformed matrix T by applying the averaging and differencing operations, first along each row and then along each column; (c) select an appropriate thresholding method and apply it to obtain a new matrix, denoted as D; and (d) use matrix D to calculate the compression ratio and other performance measures, as well as to reconstruct the original image. Next, the effect of a single step of averaging and differencing on an image is examined. Fig 9 presents the original image, while Fig 10 illustrates the transformed image obtained after applying the averaging and differencing operations from level 1 to level 4.

## 4. Results and discussion

### 4.1 Experimental results

In this study, the compression ratio (CR) is defined as the ratio between the number of nonzero elements in the original matrix and the number of nonzero elements in the updated transformed matrix. The obtained CR values for different thresholding methods and various values of ε are presented in Table 2.

Table 2, Compression ratio results for different thresholding techniques

| ∑ | **CR(hard threshold)** | **CR(soft threshold)** |
|---|---|---|
| 15 | 15.74 | 14.1 |
| 20 | 17.11 | 15.87 |
| 25 | 18.47 | 16.95 |

The universal thresholding method produces a compression ratio (CR) of 14.375. It is observed that the hard thresholding method achieves the highest CR among the evaluated techniques. The soft thresholding method provides a better CR compared to the universal thresholding method [24]; however, its performance depends on the appropriate selection of the threshold value ε. The Peak Signal-to-Noise Ratio (PSNR) for an 8-bit grayscale image is defined as [25]:

PSNR (dB) = 20 log10 $(\frac{255}{\sqrt{\text{MSE}}})$, where MSE is the Man Squared Error defined by:

MSE= $\frac{1}{mn}\sum_{y=1}^{m}\sum_{x=1}^{n}(I(x,y)-I^{1}(x,y))^{2}$, where, I is original image, $I^{1}$ is approximation of decompressed image and m; n are dimensions of the image.

The PSNR values obtained for different threshold values and thresholding techniques are presented in Fig. 10 (Level 3). The results indicate that the soft thresholding method provides better PSNR performance compared with the hard thresholding method [24,25]. The universal thresholding method achieves a PSNR value of 24.875.

The results presented in Fig. 8 are acceptable for most applications; however, they may not be suitable for medical applications where complete preservation of image information is required. Furthermore, PSNR alone is not an adequate perceptual measure of image quality because reconstruction errors do not generally behave like signal-independent additive noise [26,27], and the severity of visual distortions cannot always be accurately represented through simple power measurements. In some cases, a small amount of image degradation may result in a low PSNR value, even though the perceived image quality remains acceptable.

Therefore, perceptual quality assessment methods based on Mean Opinion Score (MOS) and Picture Quality Scale (PQS) are applied [26,27] to provide a more meaningful evaluation. The reference and test conditions are arranged in pairs, where the first represents the original unimpaired reference image and the second represents the corresponding compressed image with introduced impairments. The original uncompressed image is used as the reference condition for comparison.

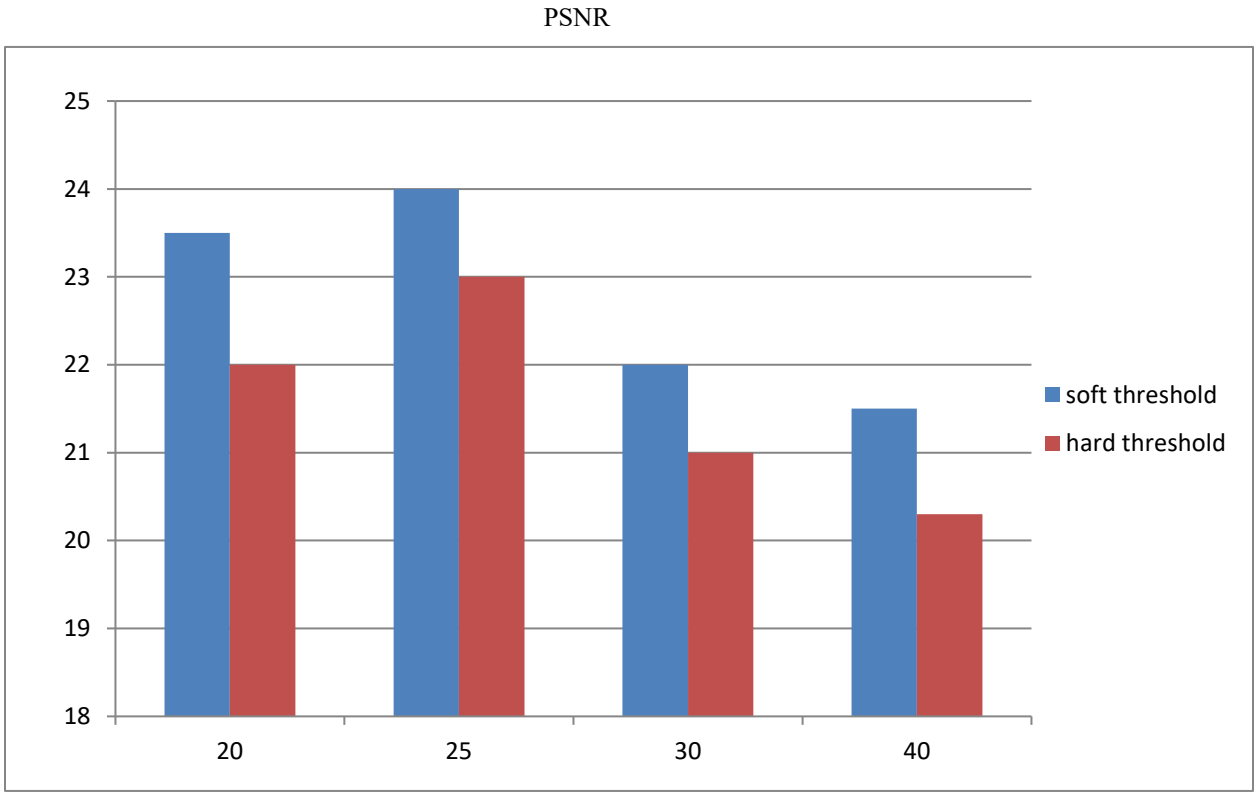



Fig.8 Comparison of PSNR values for different thresholding techniques

The method employs a five-grade impairment scale consisting of the following ratings; 5 (excellent), 4 (good), 3 (slightly annoying), 2 (annoying), and 1 (very annoying). The Mean Opinion Score (MOS) considers relevant characteristics of the human visual system (HVS) [27], particularly for evaluating global image impairments such as random errors, while giving greater emphasis to the perceptual significance of structured and localized distortions.

In this study, a linear combination of uncorrelated principal distortion measures (Zi), weighted by partial regression coefficients (bi), is applied. The Picture Quality Score (PQS) is then developed through regression analysis using the MOS values. The obtained MOS and PQS values are presented in Table 3, and the results demonstrate encouraging performance.

Table 3, Mean opinion score (MOS) and perceptual quality score (PQS) evaluation of compressed images

| **ε=15** | **MOS** | **PQS** |
|---|---|---|
| Hard Thresholding | 4.675 | 4.765 |
| Soft Thresholding | 4.80 | 4.875 |
| Universal<br><br>Thresholding | 4.865 | 4.957 |

Initially, the source image shown in Fig. 9 was loaded into the MATLAB working environment using the developed source code. The implemented code performs the 2D Haar Wavelet transformation and compression process.

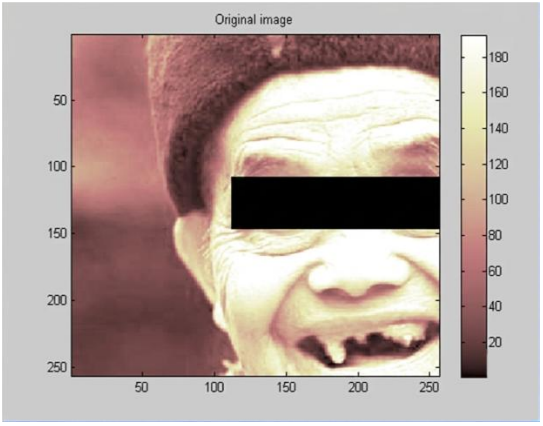



Fig.9 Original dental image used as the input for Haar wavelet compression

Subsequently, consecutive wavelet compression is performed using different levels of decomposition. The results obtained for four different levels of wavelet decomposition are presented in Fig. 10.

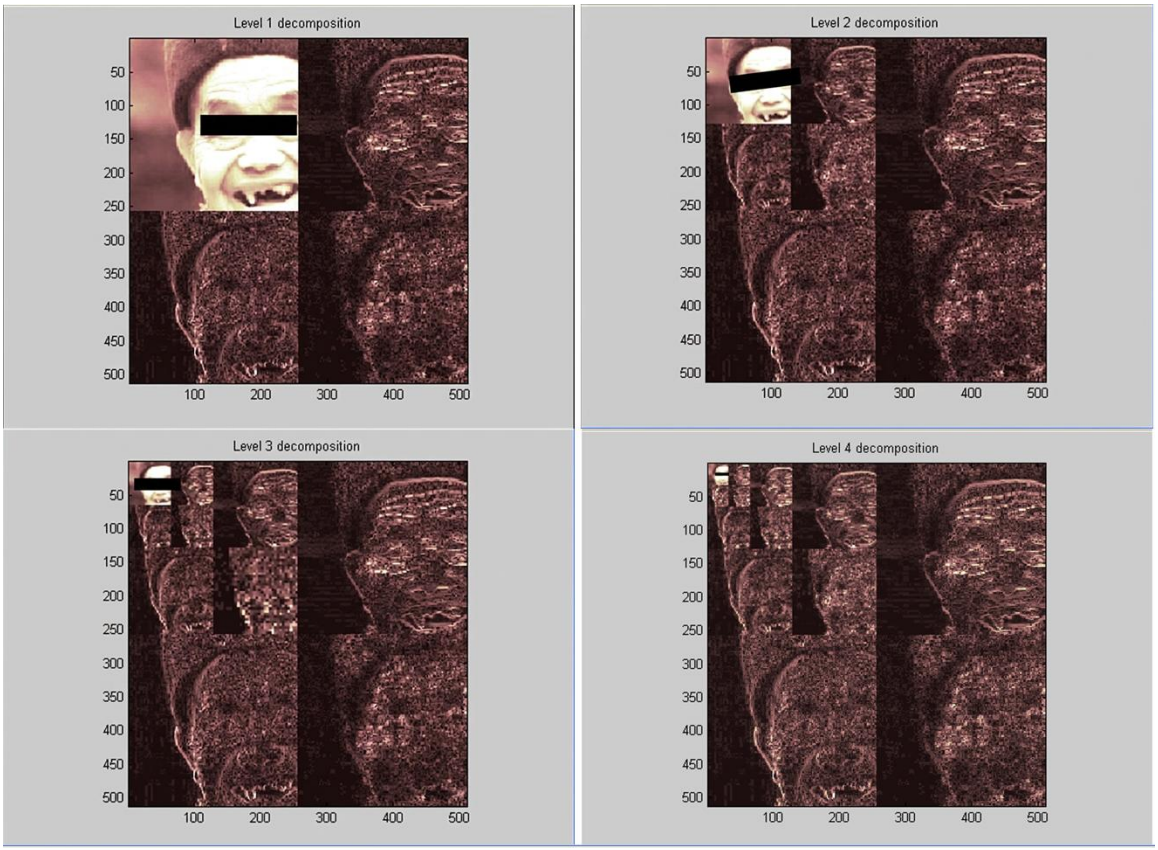



Fig.10 the four decomposition results obtained at different levels using the Haar wavelet transform

**4.2 Discussion**

The experimental results demonstrate that the performance of Haar wavelet-based image compression is strongly influenced by the decomposition level and the selected threshold value. Increasing the number of wavelet decomposition levels improves the ability of the transform [24,28] to separate significant image information from less important details. Consequently, more insignificant wavelet coefficients can be discarded while preserving the essential visual characteristics of the reconstructed image. This multiresolution property enables efficient image compression with acceptable reconstruction quality.

Compression in the proposed method is achieved through wavelet coefficient thresholding [24]. Three thresholding techniques; hard thresholding, soft thresholding, and universal thresholding, were investigated to determine their influence on compression performance. Coefficients with magnitudes below a predefined threshold are removed, thereby reducing the amount of information required to represent the image. As the threshold increases, the compression ratio improves because more coefficients are discarded. However,

excessive thresholding [24,28] also removes useful image information, resulting in reduced reconstruction quality.

The proposed compression algorithm was evaluated under two operating conditions. In the first mode, the compression ratio (CR) was specified, and the threshold value was adjusted until the desired compression ratio was achieved. The Peak Signal-to-Noise Ratio (PSNR) of the reconstructed image was then calculated to assess image quality. In the second mode, the desired PSNR was fixed, and the threshold value was varied until the required image quality was obtained, after which the corresponding compression ratio was determined. These two evaluation modes provide insight into the trade-off between compression efficiency and reconstructed image quality.

The experimental observations indicate that increasing the decomposition level generally improves image quality [28] because the wavelet transform provides a more effective separation of low-frequency image content from high-frequency details. Nevertheless, additional decomposition levels increase computational complexity and reduce coding efficiency. Furthermore, PSNR tends to reach a saturation point beyond a certain decomposition level, indicating that further decomposition provides only marginal improvements in reconstructed image quality. For each compression ratio, an optimal decomposition level exists at which PSNR reaches its maximum value. Beyond this point, image quality gradually deteriorates due to the loss of important wavelet coefficients. These findings suggest that adaptive selection of the decomposition level is essential for achieving an appropriate balance between compression performance and computational cost.

Compression performance was primarily evaluated using objective quality metrics, including Compression Ratio (CR), Mean Square Error (MSE), Peak Signal-to-Noise Ratio (PSNR), and Picture Quality Scale (PQS). Although MSE and PSNR remain the most widely used quantitative measures because of their computational simplicity, they do not always correlate well with perceived visual quality [26,27]. Human observers evaluate reconstructed images [27] based on characteristics such as edge preservation, texture continuity, smoothness, and the visibility of compression artifacts rather than on pixel-wise differences alone. Consequently, perceptual quality assessment methods based on characteristics of the Human Visual System (HVS), including Mean Opinion Score (MOS) and Picture Quality Scale (PQS), provide complementary information regarding the visual fidelity of compressed images. The encouraging PQS results obtained in this study indicate that the proposed Haar wavelet compression method preserves perceptually important image information while achieving satisfactory compression performance.

The proposed framework can also be extended to color image compression [29]. Instead of processing RGB components directly, the image may first be transformed into the YIQ or a similar luminance–chrominance color space. Since the Human Visual System is considerably more sensitive to luminance variations [29,30] than chrominance information, larger compression errors can be tolerated in the chrominance channels without noticeably affecting perceived image quality. This approach can further improve compression efficiency while maintaining satisfactory visual appearance.

So, the experimental results confirm that the Haar wavelet provides an effective and computationally efficient solution for two-dimensional image compression. The proposed method achieves a favorable balance between compression ratio and reconstructed image quality while maintaining relatively low computational complexity. This makes the approach suitable for applications requiring efficient image storage and transmission, including medical imaging, multimedia systems, and web-based image services.

Despite these promising results, several opportunities exist for further improvement. Future research may investigate adaptive threshold selection strategies that automatically determine the optimal threshold value according to image characteristics. In addition, adaptive decomposition level selection could improve the balance between computational complexity and compression performance.

## 5. Conclusions

This study presented a two-dimensional (2D) image compression method based on the Haar Discrete Wavelet Transform (DWT). The proposed approach exploits the multiresolution characteristics of the Haar wavelet to decompose an image into approximation and detail coefficients, enabling efficient data reduction while preserving important visual information. The reconstructed images were evaluated using widely accepted performance metrics, demonstrating that the proposed method achieves effective compression while maintaining acceptable reconstructed image quality.

The experimental analysis indicates that compression performance is strongly influenced by the decomposition level and the selected threshold value. Higher decomposition levels generally improve the separation of significant and insignificant wavelet coefficients, resulting in better image quality. However, increasing the decomposition level also raises computational complexity and eventually yields diminishing improvements in reconstruction quality. These observations highlight the importance of selecting appropriate decomposition levels and threshold values to achieve a practical balance between compression efficiency and visual fidelity.

The computational complexity and efficient reconstruction capability of the Haar wavelet make it a suitable choice for applications requiring fast image compression, including multimedia systems, web-based image transmission, and medical image storage. Although more advanced wavelet families may achieve higher compression efficiency, the Haar wavelet remains an attractive solution for resource-constrained environments because of its ease of implementation and computational efficiency.

Additional research should investigate adaptive decomposition level selection, comparative evaluations with other wavelet families and the incorporation of more advanced perceptual image quality assessment metrics. Furthermore, validating the proposed method on larger benchmark datasets and application-specific image collections, particularly in medical imaging, will provide a more comprehensive assessment of its effectiveness and practical applicability.

## 6. Competing interests

We declare that all the authors have no competing interests.

## 7. Declarations

7.1 Ethical approval: NOT APPLICABLE

7.2. Accordance: NOT APPLICABLE

7.3 Consent to participate: NOT APPLICABLE

7.4 Consent to publish: NOT APPLICABLE

## 8. Data availability

All data generated and analyzed during the research are included within this paper and Science Data Bank with a full name of the database “Optimizing Physiological Image Compression via Discrete Wavelet Transform without Loss of Clinical Relevance”, and DOI https://doi.org/10.57760/sciencedb.42758 or link https://cstr.cn/31253.11.sciencedb.42758.

**9. Funding:** NOT APPLICABLE

## 10. Author contribution

Dawit Teklu Weldeslasie and Tedros Kebede Bidada contributed to the conceptualization, methodology, algorithm development, data curation, and formal analysis of the study. Yayneshet Tadele Aynalem was responsible for the validation and resources. All authors critically reviewed, edited and provided final approval for the published version.

## References

[1]. Bourai, N.E.H., Merouani, H.F. & Djebbar, A. Deep learning-assisted medical image compression challenges and opportunities: systematic review. *Neural Comput & Applic* 36, 10067–10108 (2024). https://doi.org/10.1007/s00521-024-09660-8
[2]. Rao, S.V.B.S., Rao, T.S., Sowjanya, M. *et al.* Deep learning and traditional methods for remote sensing image analysis. *Discov. Imaging* 3, 5 (2026). https://doi.org/10.1007/s44352-026-00027-4
[3]. Devadason, J.R., D, A. A comprehensive survey of image compression methods: from prediction models to advanced techniques. *Multimed Tools Appl* 84, 38653–38691 (2025). https://doi.org/10.1007/s11042-025-20687-4
[4]. Seeli, D.J.J., Thanammal, K.K. A comparative review and analysis of medical image encryption and compression techniques. *Multimed Tools Appl* 84, 4457–4473 (2025). https://doi.org/10.1007/s11042-024-18745-4
[5]. Roshan, R., Aghazadeh, N. & Farajzadeh, N. Enhanced image compression using wavelet-based encoder-decoder architectures. *SIViP* 20, 117 (2026). https://doi.org/10.1007/s11760-026-05134-7
[6]. Cardozo, A., da Rosa, M.M.A., Seidel, H. *et al.* A Power-Efficient Approximate Multi-Level Discrete Haar Wavelet Transform Design for ECG Data Compression. *Circuits Syst Signal Process* (2026). https://doi.org/10.1007/s00034-026-03545-y
[7]. Mathuria, M., Saini, D.K. (2025). Advances in Image Processing and Pattern Recognition. In: Nema, R., Kumar, A., Saini, D.K. (eds) Advances in Cancer Detection, Prediction, and Prognosis Using Artificial Intelligence and Machine Learning. Springer, Singapore. https://doi.org/10.1007/978-981-96-9346-7_5
[8]. Seeli, D.J.J., Thanammal, K.K. A comparative review and analysis of medical image encryption and compression techniques. *Multimed Tools Appl* 84, 4457–4473 (2025). https://doi.org/10.1007/s11042-024-18745-4

[9]. Dai, F. Deep learning based medical image compression using cross attention learning and wavelet transform. *Sci Rep* 15, 40008 (2025). https://doi.org/10.1038/s41598-025-23582-y
[10]. Ruosch, F., Rossetto, L. (2026). Applications of Multimodal Knowledge Graphs in Modeling Multimedia. In: Lokoč, J., *et al.* MultiMedia Modeling. MMM 2026. Lecture Notes in Computer Science, vol 16412. Springer, Singapore. https://doi.org/10.1007/978-981-95-6950-2_45
[11]. Kanwal, S., Tao, F., Taj, R. *et al.* Discrete cosine transform and discrete wavelet transform based hybrid method for robust and blind medical image watermarking. *Peer-to-Peer Netw. Appl.* 18, 251 (2025). https://doi.org/10.1007/s12083-025-02059-9
[12]. Anitha, R., Sridevi, S. Hybrid approximate multiplier architectures for low power DWT image compression. *Sci Rep* 16, 21622 (2026). https://doi.org/10.1038/s41598-026-54818-0
[13]. Zhu, K., Fuh, YH.J. (2026). Digital Image Processing. In: Monitoring and Control of Laser Additive Manufacturing Process. Additive Manufacturing Technology. Springer, Singapore. https://doi.org/10.1007/978-981-95-5226-9_7
[14]. Khan, A.A., Laghari, A.A., Inam, S.A. *et al.* A survey on multimedia-enabled deepfake detection: state-of-the-art tools and techniques, emerging trends, current challenges & limitations, and future directions. *Discov Computing* 28, 48 (2025). https://doi.org/10.1007/s10791-025-09550-0
[15]. C-Rella, J., Vilar, J.M. Flexible multi-class cost-sensitive thresholding. *Adv Data Anal Classif* (2025). https://doi.org/10.1007/s11634-025-00651-8
[16]. Samantaray, A.K., Rahulkar, A.D. (2024). Fundamentals of Wavelet Filter Banks. In: Feature Extraction in Medical Image Retrieval. Springer, Cham. https://doi.org/10.1007/978-3-031-57279-1_2
[17]. Dantas, P.V., Sabino da Silva, W., Cordeiro, L.C. *et al.* A comprehensive review of model compression techniques in machine learning. *Appl Intell* 54, 11804–11844 (2024). https://doi.org/10.1007/s10489-024-05747-w
[18]. Xu, Y., Khan, T.M., Song, Y. *et al.* Edge deep learning in computer vision and medical diagnostics: a comprehensive survey. *Artif Intell Rev* 58, 93 (2025). https://doi.org/10.1007/s10462-024-11033-5
[19]. Kim, KI., Pak, MI., Ri, YG. *et al.* An image compression method for improving noise robustness of ultrasonic medical image compression in wavelet domain. *Multimed Tools Appl* 84, 45453–45478 (2025). https://doi.org/10.1007/s11042-025-20943-7
[20]. Majhi, M., Mallick, A.K. A comprehensive survey of content based image retrieval schemes: advancements, challenges, and future directions. *Multimed Tools Appl* 85, 178 (2026). https://doi.org/10.1007/s11042-026-21337-z
[21]. Harshitha, S., Mahadevaswamy, U.B. (2025). Review of Digital and Medical Image-Based Compression Techniques. In: Kumar, R., Verma, A.K., Verma, O.P., Rajpurohit, J. (eds) Soft Computing: Theories and Applications. SoCTA 2024. Lecture Notes in Networks and Systems, vol 1344. Springer, Singapore. https://doi.org/10.1007/978-981-96-5958-6_3
[22]. Harshitha, S., Mahadevaswamy, U.B. (2025). Review of Digital and Medical Image-Based Compression Techniques. In: Kumar, R., Verma, A.K., Verma, O.P., Rajpurohit, J. (eds) Soft Computing: Theories and Applications. SoCTA 2024. Lecture Notes in Networks and Systems, vol 1344. Springer, Singapore. https://doi.org/10.1007/978-981-96-5958-6_3
[23]. Lee, D., Han, J.H., Yong, TH. *et al.* Structure-aware efficient compression for dental image segmentation using differentiable gates and masked knowledge distillation. *Multimed Tools Appl* 85, 253 (2026). https://doi.org/10.1007/s11042-026-21462-9
[24]. Liang, P. *et al.* (2026). Vision Foundation Models in Medical Image Analysis: Advances and Challenges. In: Chen, J., Luo, X., Yu, Y. (eds) Blockchain and Trustworthy Systems. BlockSys 2025. Communications in Computer and Information Science, vol 2638 . Springer, Singapore. https://doi.org/10.1007/978-981-95-3483-8_13
[25]. Pathak, K., Bhandari, A.K. Advances in Deep Learning and Filtering Models for Medical Image Denoising: A Review of Current and Future Trends. *Circuits Syst Signal Process* (2026). https://doi.org/10.1007/s00034-025-03477-z
[26]. Wu, X., Shi, Z. A comprehensive features representation for no-reference image quality assessment. *Multimedia Systems* 31, 403 (2025). https://doi.org/10.1007/s00530-025-02016-9
[27]. Ji, W., Chen, X. Blind image quality assessment based on statistical features. *Sci Rep* 16, 14756 (2026). https://doi.org/10.1038/s41598-026-42799-z
[28]. Zouari, S., Ghazalah, S.A., Masmoudi, A. *et al.* Enhancing lossless image compression with Bayesian mixture models and spatial domain encoding. *SIViP* 19, 1438 (2025). https://doi.org/10.1007/s11760-025-05030-6
[29]. Ji, X., Yang, X., Yue, Z. *et al.* Deep Learning Image Compression Method Based On Efficient Channel-Time Attention Module. *Sci Rep* 15, 15678 (2025). https://doi.org/10.1038/s41598-025-00566-6
[30]. Orban, G.A., Urgen, B.A. (2025). Functional Imaging of the Human Visual System. In: Filippi, M. (eds) fMRI Techniques and Protocols. Neuromethods, vol 220. Humana, New York, NY. https://doi.org/10.1007/978-1-0716-4438-6_19